Spin reorientation and magnetohistory of $DyFe_{12-x}Nb_x$ compounds

2001 J. Phys.: Condens. Matter 13 1733

(http://iopscience.iop.org/0953-8984/13/8/310)

INSTITUTE OF PHYSICS PUBLISHING JOURNAL OF PHYSICS: CONDENSED MATTER

J. Phys.: Condens. Matter **13** (2001) 1733–1741 www.iop.org/Journals/cm PII: S0953-8984(01)15770-X

Spin reorientation and magnetohistory of $DyFe_{12-x}Nb_x$ compounds

J L Wang, Y P Shen, C P Yang, N Tang, B Fuquan, D Yang, G H Wu and F M Yang

State Key Laboratory of Magnetism, Institute of Physics, Chinese Academy of Sciences, PO Box 603, Beijing 100080, People's Republic of China

Received 25 July 2000, in final form 8 January 2001

Abstract

Structural and magnetic properties, especially the magnetocrystalline anisotropy of $DyFe_{12-x}Nb_x$ compounds with $x = 0.55$–0.85, have been investigated. The easy magnetization directions at room temperature for all the compounds are along the c-axis. With decreasing temperature the magnetocrystalline anisotropy changes from easy axis to easy cone at T_{sr2}, then to easy plane at T_{sr1}. A spin phase diagram has been constructed for $DyFe_{12-x}Nb_x$. The change of magnetocrystalline anisotropy was further investigated by the angular dependence of magnetization with respect to the magnetic field at various temperatures. The temperature dependence of the cone angle was determined for $DyFe_{11.3}Nb_{0.7}$. It is noteworthy that with increasing Nb content both T_{sr1} and T_{sr2} decrease monotonically while the Curie temperature is almost independent of Nb content. The cone angle increases monotonically with decreasing temperature from T_{sr2} and discontinuously comes up to 90° at T_{sr1}. The temperature dependence of the cone angle can be quite well defined in terms of crystal field theory. In addition, an obvious magnetohistory effect was observed for all compounds at low temperature. The critical field of magnetohistory was found to be smaller than 0.5 T for $DyFe_{11.3}Nb_{0.7}$.

1. Introduction

Since Sun and Coey [1] reported that the introduction of nitrogen to some R–Fe-based compounds could lead to a dramatic improvement of hard-magnetic properties, the Fe-rich rare-earth (R) transition-metal (T) nitrides or carbides have attracted much attention. The investigation of magnetic and structural properties of the $ThMn_{12}$-type R–T compounds and their nitrides becomes a hot-point in the search for novel permanent-magnet materials since some of them exhibit excellent permanent-magnet properties [2]. In order to improve further the magnetic performances of the R–T interstitial compounds, it is necessary to achieve a further fundamental understanding of the magnetic properties of the parent alloys. Recently, it has been found that the stabilizing element not only plays an important role to stabilize the

0953-8984/01/081733+09$30.00

$ThMn_{12}$-type structure, but also influences magnetic properties, especially anisotropy of the compounds [3]. For the $DyFe_{12-x}M_x$ compounds with M = Mo [4], Ti [5–7], V [8], Si [9], Nb [10], Ta [11] and Cr [12], it was reported that the type of anisotropy is different for various M elements and the spin reorientation temperature shows a larger difference in the different references even for the same M element. As an example, T_{sr1} and T_{sr2} are 58 K and 200 K in [5] while they are 120 and 220 K in [7]. In order to get a fundamental understanding of the difference, in this paper attention is paid to the investigation of the influence of Nb content on structural and magnetic properties, especially the magnetocrystalline anisotropy of $DyFe_{12-x}Nb_x$ compounds.

2. Experimental process

The alloys of $DyFe_{12-x}Nb_x$ with x from 0.5 to 0.85 were prepared by arc-melting the starting materials with purity equal to or higher than 99.9%. The ingots were remelted at least three times to promote homogeneity. An appropriate excess amount of R was added to compensate the weight loss of the R element during melting. Structure and phase composition of the obtained samples were checked by x-ray diffraction (XRD) measurements and thermomagnetic analysis (TMA). XRD patterns on magnetically aligned powder samples obtained at room temperature were used to determine the easy magnetization direction (EMD) of the compounds. TMA in a low field of 0.05 T was performed from 4.2 K to room temperature by use of a SQUID magnetometer and from room temperature to above the Curie temperature by a vibrating-sample magnetometer. Magnetization curves were measured in an extracting-sample magnetometer in fields up to 7 T.

3. Results and discussion

Both XRD patterns of the randomly oriented powder samples and TMA of bulk samples indicate that single-phase $DyFe_{12-x}Nb_x$ compounds with $ThMn_{12}$-type structure were obtained for x ranging from 0.60 to 0.85. For $x \geqslant 0.85$ and $x \leqslant 0.60$ samples, some impurity phases, i.e. α-Fe and $NbFe_2$ and 2:17 phase appear. The lattice parameters were derived from XRD patterns of randomly oriented powder samples. It was found that with increasing Nb content the unit cell volume increases slightly due to larger radius of Nb than Fe.

The Curie temperatures T_C were determined to be 518($\pm$5) K by M^2–T plots and extrapolating M_2 to zero. The value of T_C has almost no change with increasing Nb content. It is well known that in the Fe-rich R–Fe compounds the Curie temperature is mainly determined by the exchange interaction J_{Fe-Fe} between the Fe moments. The experimental results indicate that the exchange interaction is almost independent of Nb content, similar to the case in the $YFe_{12-x}Ti_x$ compounds [13].

The saturation magnetizations M_s at 5 K and room temperature were derived from M–$1/B$ curves and by extrapolating $1/B$ to zero as shown in figure 1. It can be seen that M_s decreases monotonically with increasing x and the values of M_s at 5 K are lower than those at room temperature due to the ferrimagnetic coupling between Dy and Fe moments. On the other hand, the speed of decrease of M_s with Nb content is much faster than that expected by a simple dilution model (see the dashed line in figure 1). The site occupation of the stabilizing element M in the $RT_{12-x}M_x$ compounds can be analysed in terms of combination of the metallic radius and the heat of mixing between R and M atoms as has been done by Buschow and de Mooij [14]. In the $RFe_{12-x}M_x$ compounds Fe atoms occupy three non-equivalent sites: 8i, 8j and 8f. The average distance of Fe–Fe pairs at different sites shows the following relationship:

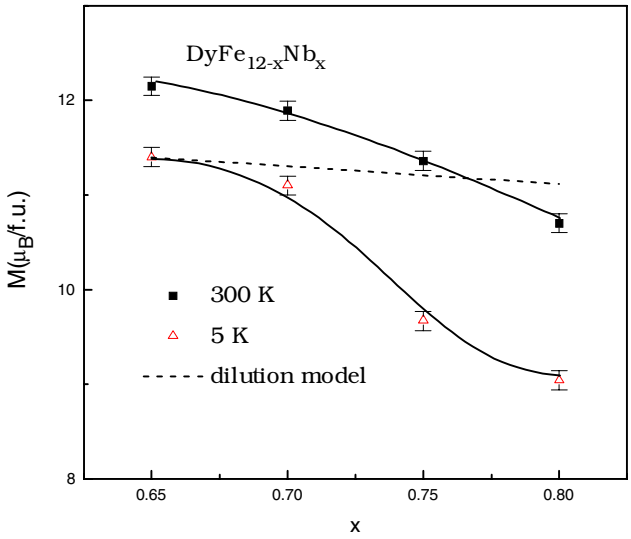

Figure 1. Composition dependence of saturation magnetization at 5 K and 300 K of $DyFe_{12-x}Nb_x$ compounds.

$d_{FeFe}(8i) > d_{FeFe}(8j) > d_{FeFe}(8f)$. On the basis of average Fe–Fe distances, it may be expected that the Nb atoms prefer to occupy the 8i site instead of the 8f or 8j sites because Nb atoms have larger atomic radius than Fe atoms, which has been confirmed by the neutron diffraction result [15]. It was accepted that the moments at the non-equivalent Fe sites hold the following relationship: $\mu_{Fe}(8i) > \mu_{Fe}(8j) > \mu_{Fe}(8f)$. So the preferential occupation on 8i of Nb atoms may be responsible for the faster decrease of M_s.

The XRD patterns of the magnetically aligned powder samples show that all compounds investigated exhibit easy-axis anisotropy at room temperature. Figure 2 shows the temperature dependences of magnetization at a low field of 0.1 T. It can be seen that there are two anomalies in the M–T curves. The temperature dependence of ac susceptibility also indicates these anomalies at the same critical temperatures. In order to check what happens at the critical temperature at which the anomaly occurs, the magnetization curves of the magnetically aligned samples were measured at various temperatures with an external field applied parallel and perpendicular to the alignment direction, respectively. Figure 3 shows the magnetization curves of $DyFe_{12-x}Nb_x$ compounds with $x = 0.65$, 0.7, 0.75 and 0.80. It can be seen that the anisotropy of these compounds changes with decreasing temperature: the c-axis that is the EMD at room temperature becomes the hard magnetization direction (HMD) at 5 K. What kind of anisotropy does the compound exhibit between the two critical temperatures? In order to make this question clear, we measured the dependence of magnetization of the magnetically-aligned powder sample on the angle θ between the alignment direction and the external field at various temperatures. Generally, if the anisotropy type is of easy axis or easy plane, there exists one maximum between 0° and 180° in the M–θ curve while two maxima appear at θ_{max1} and θ_{max2}, respectively, for the easy-cone type of anisotropy. The cone angle α can be derived by $\alpha = (\theta_{max2} - \theta_{max1})/2$. As an example, figure 4 shows the dependence of magnetization of the magnetically-aligned powder sample for the $DyFe_{11.25}Nb_{0.75}$ compound on the angle α between the alignment direction and the external field at various temperatures. It can be seen that at 300 K the EMD is along the c-axis and it lies in the ab-plane at 5 K while the type of

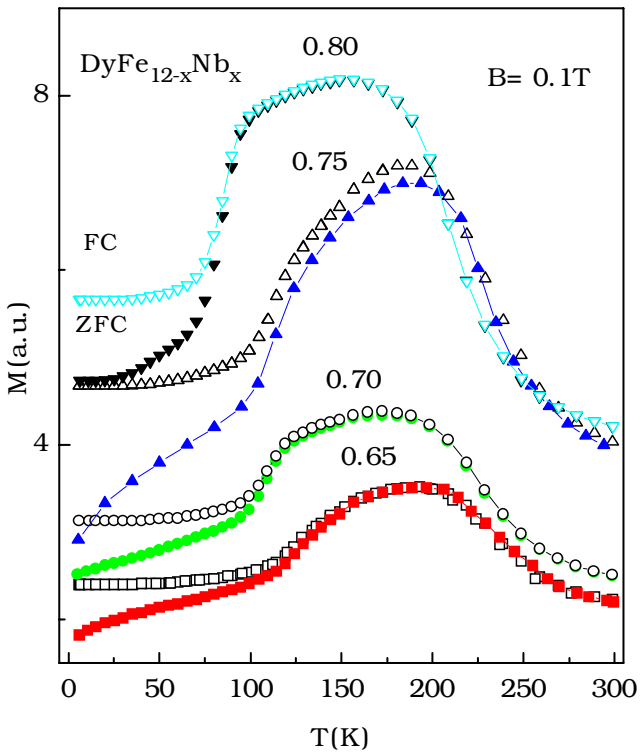

Figure 2. Temperature dependence of magnetization measured upon zero-field cooling (ZFC) and field cooling (FC) for $DyFe_{12-x}Nb_x$ compounds in a field of 0.1 T.

anisotropy is easy cone at 125 K and 150 K. So it is clear that the anomalies in the M–T or χ–T curves correspond to the spin reorientations. The spin reorientation temperatures T_{sr1} and T_{sr2} (T_{sr1} and T_{sr2} correspond to lower and higher temperature anomalies, respectively, within the experimental accuracy of ± 5 K) were derived from the peaks in the $\mathrm{d}M/\mathrm{d}T$ curves, which are in good agreement with the values determined by the peaks in the χ–T curves. By using the obtained spin reorientation temperatures T_{sr1} and T_{sr2} a spin phase diagram has been constructed for $DyFe_{12-x}Nb_x$ compounds as shown in figure 5. It can be seen that the EMD is along the c-axis between T_{sr2} and T_C. With decreasing temperature, the EMD begins to deviate from the c-axis at T_{sr2} and becomes a cone around the c-axis between T_{sr1} and T_{sr2}. When $T < T_{sr1}$, the EMD comes to the basal plane. It is noteworthy that in contrast to the Curie temperature, both T_{sr1} and T_{sr2} show a remarkable decrease with increasing Nb content even for a small change range of Nb content. The temperature dependence of α is shown in figure 6 for the $DyFe_{11.3}Nb_{0.7}$ compound. The cone angle α increases smoothly from T_{sr2} up to T_{sr1} with decreasing temperature. However, at T_{sr1} the cone angle discontinuously increases from about 54° to 90°, which means the EMD lies in the ab-plane below T_{sr1}. Andreev *et al* [16] have found that the external field has a dramatic influence on the spin reorientation temperature T_{sr} for $TbFe_{11}Ti$. Here it was found the stabilizing element content has a remarkable influence on the spin reorientation temperatures.

It is accepted that the anisotropy of the rare-earth sublattice with tetragonal symmetry may be expressed as

$$E_a^R = K_1(R)\sin^2\theta + (K_2(R) + K_2'(R)\cos 4\phi)\sin^4\theta + (K_3(R) + K_3'(R)\cos 4\phi)\sin^6\theta \qquad (1)$$

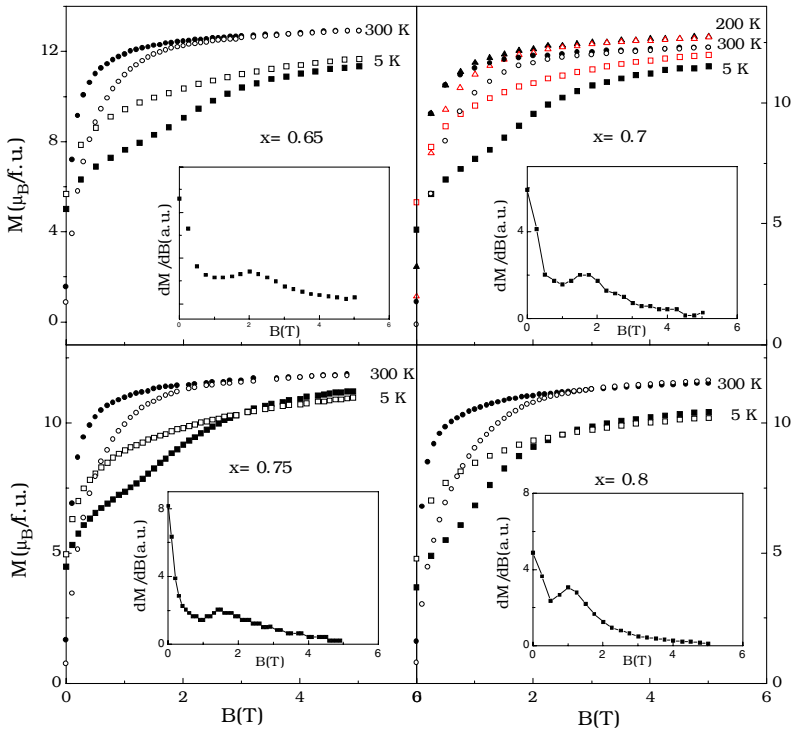

Figure 3. Magnetization curves of $DyFe_{12-x}Nb_x$ compounds at 5 K and 300 K measured along and perpendicular to the aligned direction. The inset draws dM/dB at 5 K for the HMD.

where θ, ϕ are the polar angles and azimuth of the magnetization vector, respectively, in the reference frame with x parallel to [100] and z parallel to [001]. The relations between K_i for the rare-earth and the crystal-field parameters B_{nm} can be obtained by a rotation transformation of the crystal-field terms as follows:

$$\begin{aligned}
K_1(R) &= -[\tfrac{3}{2}B_{20}\langle O_{20}\rangle + 5B_{40}\langle O_{40}\rangle + \tfrac{21}{2}B_{60}\langle O_{60}\rangle] \\
K_2(R) &= \tfrac{7}{8}[5B_{40}\langle O_{40}\rangle + 27B_{60}\langle O_{60}\rangle] \\
K_2'(R) &= \tfrac{1}{8}[B_{44}\langle O_{40}\rangle + 5B_{64}\langle O_{60}\rangle] \\
K_3(R) &= -\tfrac{231}{16}B_{60}\langle O_{60}\rangle \\
K_3'(R) &= -\tfrac{11}{16}B_{64}\langle O_{60}\rangle
\end{aligned} \tag{2}$$

where $\{\langle O_{nm}\rangle\}$ are thermal average values of the matrix elements of Stevens operator equivalents. Generally, it is well accepted that the $\langle O_{nm}\rangle$ values vary with temperature as the $n(n+1)/2$ power of the R sublattice magnetization M_R [17] and the intersublattice coupling between R and T moments keeps M_R at a sufficiently high level even at elevated temperatures due to the weakness of J_{RR} compared with J_{RT} and J_{TT}. The 3d magnetic moment and anisotropy are roughly independent of temperature when the temperature is much lower than the ordering temperature. At low temperature the R-sublattice anisotropy is dominant. With increasing temperature the R-sublattice anisotropy decreases and the T-sublattice contribution to anisotropy becomes dominant.

The magnetization direction in the compounds is determined by minimizing the anisotropy energy $E_a^{tot} = K_1(\mathrm{Fe})\sin^2\theta + E_a^R$, in which the factor of the rare-earth atom number per

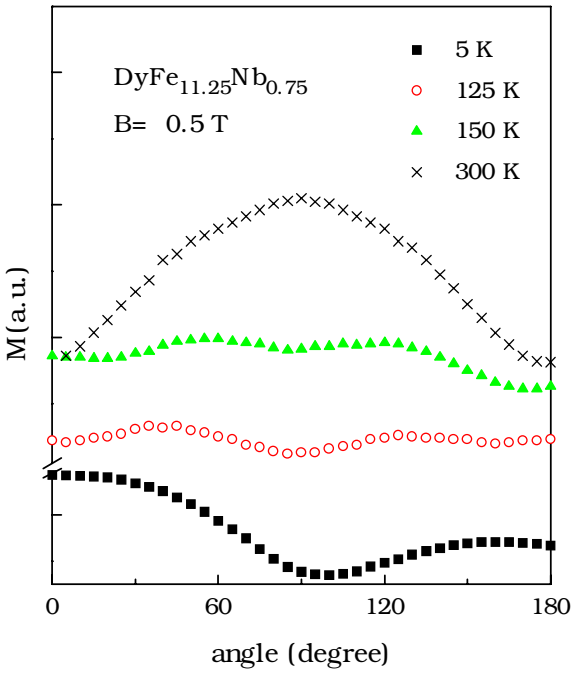

Figure 4. Dependence of the magnetization of $DyFe_{11.25}Nb_{0.75}$ compound on the angle between the alignment direction and the direction of the external field of 0.5 T.

formula in front of E_a^R has been put as 1 for the 1:12 structure. In the plane containing the c-axis the anisotropy depends on K_1(Fe), K_i(R) ($i = 1, 2, 3$) and $K_i(\mathrm{R})'$ ($i = 2, 3$), while in the plane perpendicular to the c-axis the anisotropy depends only on $K_i(\mathrm{R})'$ ($i = 2, 3$). The mixing effects of K_1(Fe), K_i(R) and $K_i(\mathrm{R})'$ give the tilting angle and $K_i(\mathrm{R})'$ determines the angular component in this plane. By fitting M–T curves, the temperature dependence of M_R was obtained using the molecular-field theory. The temperature dependence of K_1(Fe) was obtained from the measurements for corresponding $YFe_{12-x}Nb_x$ compounds. Taking the five crystal-field parameters $\{B_{nm}\}$ as the same as those of a $DyFe_{11}Ti$ single crystal [13], $B_{20} = 0.160$ K, $B_{40} = 11.0 \times 10^{-4}$ K, $B_{44} = -105 \times 10^{-4}$ K, $B_{60} = 16.0 \times 10^{-6}$ K, $B_{64} = 4.0 \times 10^{-6}$ K, the temperature dependence of the angle between the EMD and the c-axis was calculated for the $DyFe_{11.3}Nb_{0.7}$ compound as shown in figure 6 (T_{sr} within the experimental accuracy of ± 5 K). It can be seen that the theoretical result is in agreement with the experimental data. The discrepancy of T_{sr} in figure 6 between the calculated and experimental data can be understood if we consider the experimental accuracy of T_{sr} and the influence due to neglecting the possible difference of the crystal-field parameters B_{nm} in $DyFe_{11}Ti$ and $DyFe_{11.3}Nb_{0.7}$. Moreover, one also finds that the EMD in the ab-plane is along the (100) direction.

It can also be seen from figure 3 that at 5 K a discontinuous jump occurs in the magnetization curves along the HMD, which is well known as the first-order magnetization process (FOMP). The values of the critical field B_{cr} of the FOMP can be determined from the peak in the $\mathrm{d}M/\mathrm{d}B$ curve as shown in the inset in figure 3. It has been found that the values of B_{cr} decrease with increasing Nb content from 2.0 T for $x = 0.65$ to 1.0 T for $x = 0.80$.

Figure 2 draws the thermomagnetic curves at a field of 0.1 T for $DyFe_{12-x}Nb_x$ compounds with $x = 0.65$, 0.70, 0.75 and 0.80 measured after a zero-field cooling (ZFC) process and a

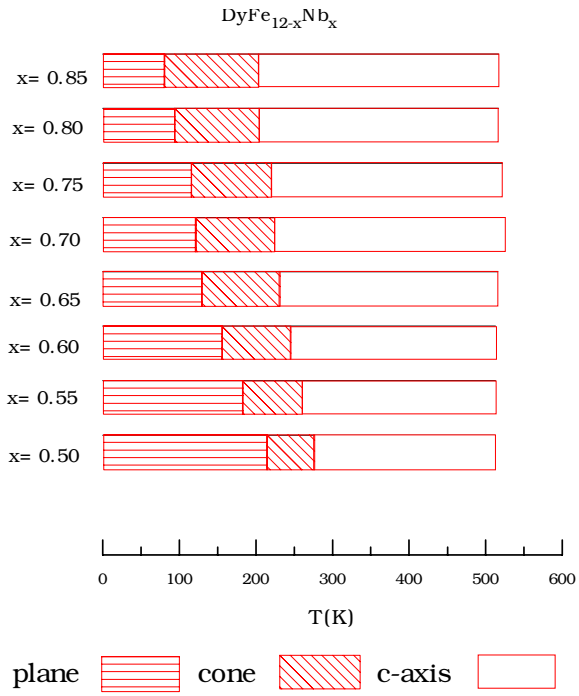

Figure 5. The spin phase diagram of $DyFe_{12-x}Nb_x$ compounds.

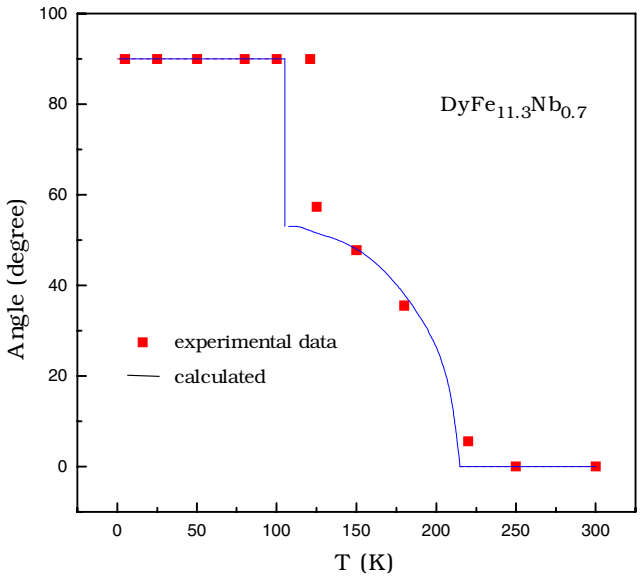

Figure 6. Experimental and theoretical temperature dependences of cone degree between the EMD and c-axis for the $DyFe_{11.3}Nb_{0.7}$ compound.

field cooling (FC) process, respectively. It can be seen that $DyFe_{12-x}Nb_x$ compounds exhibit a clear magnetohistory. According to [18], there are two possible explanations for these effects:

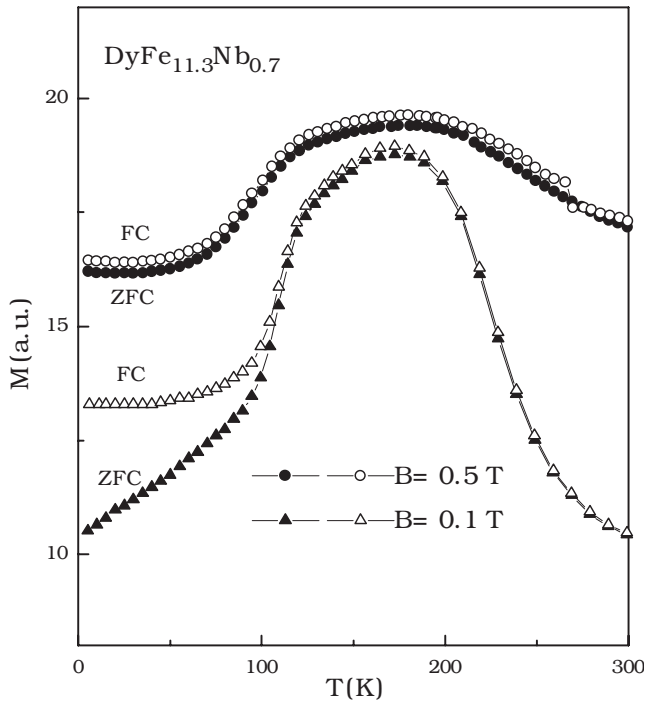

Figure 7. Temperature dependence of magnetization measured upon zero-field cooling (ZFC) and field cooling (FC) for the $DyFe_{11.3}Nb_{0.7}$ compound in a field of 0.1 and 0.5 T, respectively.

cluster glasses and narrow Bloch walls. Cluster glasses are characterized by the presence of antiferromagnetic interactions between several of the magnetic moments contained in this material, where the anisotropy of the R sublattice does not play a role. But from our experiments it appears that the anisotropy is very important to the presence of magnetohistory. So the cluster glass mechanism is not satisfactory for our case. Another possible mechanism results from the presence of narrow Bloch walls. The presence of narrow walls requires a large ratio of the anisotropy energy to the exchange energy. When the domain-wall thickness becomes of the order of a few interatomic distances, the propagation of these narrow walls needs thermal activation. With increasing temperature the energy required becomes available. For R = Y and Gd, the anisotropy only originates from the T sublattice while for R = other rare earth, the R sublattice gives a large contribution to the anisotropy, which makes the condition of presence of narrow walls satisfied. It is well accepted that the R-sublattice anisotropy energy decreases rapidly with increasing temperature. So at a certain higher temperature the condition will be broken. Figure 7 shows that the magnetohistory effects in the $DyFe_{11.3}Nb_{0.7}$ compound disappear at 0.5 T, which means that the critical field in this compound to overcome the domain wall pinning is smaller than 0.5 T.

Acknowledgments

The present investigation was supported by the National Nature Science Foundation of the People's Republic of China. J L Wang wishes to express his appreciation to Professor F R de Boer and Dr E Brück for helpful discussions.

References

[1] Coey J M D and Sun H 1990 *J. Magn. Magn. Mater.* **87** L251
[2] de Boer F R, Huang Y K, de Mooij D B and Buschow K H J 1987 *J. Less-Common. Met.* **135** 199
[3] de Boer F R, Zhao Z G and Buschow K H J 1996 *J. Magn. Magn. Mater.* **157–158** 504
[4] Yang C P, Wang Y Z, Hu B P and Wang Z X 1998 *J. Phys.: Condens. Matter* **10** 4177
[5] Christides C, Niarchos D, Kostikas A, Li H, Hu B and Coey J M D 1989 *Solid State Commun.* **72** 839
[6] Andreev A V, Bartashevich M I, Kudrevatykh N V, Razgonyaev S M, Sigaev S S and Tarasov E N 1990 *Physica* B **167** 139
[7] Garcia L M, Bartolome J, Algarabel P A, Ibarra M R and Kuzmin M D 1993 *J. Appl. Phys.* **73** 5908
[8] Drzazga Z, Winiarska A and Chelkowska G 1996 *J. Magn. Magn. Mater.* **158** 107
[9] Li Q A, Lu Y, Zhao R, Tegus O and Yang F M 1991 *J. Appl. Phys.* **70** 6116
[10] Hu B-P, Wang K-Y, Wang Y-Z, Wang Z-X and Yan Q-W 1995 *Phys. Rev.* B **51** 2905
[11] Piquer C, Artigas M, Rubin J and Bartolome J 1998 *J. Phys.: Condens. Matter* **10** 11 055
[12] Yang F M, Li Q A, Kuang J, de Boer F R, Liu J, Rao K V, Nicoladies G and Buschow K H J 1991 *J. Alloys. Compounds* **177** 93
[13] Hu B P, Li H S, Coey J M D and Gavigan J P 1990 *Phys. Rev.* B **41** 2221
[14] Buschow K H J and de Mooij D B 1989 *Concerted European Action on Magnets (CEAM)* ed I V Mitchell, J M D Coey, D Givord, I R Harris and R Hanitsch (London: Elsevier) p 63
[15] Sun X D, Yan Q W, Zhang P L, Hu B P, Wang K Y and Wang Y Z 1995 *Acta Phys. Sin.* **14** 912
[16] Andreev A V, Kudrevatykh N V, Razgonyaev S M and Tarasov E N 1993 *Physica* B **183** 379
[17] Zener C 1954 *Phys. Rev.* **96** 1335
[18] Jacobs T H and Buschow K H J 1990 *J. Less-Common. Met.* **157** L11